

The dominance of non-electron-phonon charge carrier interaction in highly-compressed superhydrides

Evgueni F. Talantsev^{1,2}

¹M.N. Mikheev Institute of Metal Physics, Ural Branch, Russian Academy of Sciences,
18, S. Kovalevskoy St., Ekaterinburg, 620108, Russia

²NANOTECH Centre, Ural Federal University, 19 Mira St., Ekaterinburg, 620002,
Russia

Abstract

Primary mechanism governed the emerge of near-room-temperature superconductivity in superhydrides is widely accepted to be the electron-phonon interaction. If so, the temperature dependent resistance, $R(T)$, in these materials should be obey the Bloch-Grüneisen equation, where the power-law exponent, p , should be equal to exact integer value of $p=5$. From other hand, there is a well-established theoretical result that the pure electron-magnon interaction should be manifested by $p=3$, and $p=2$ is the value for pure electron-electron interaction. Here we analysed the temperature dependent resistance, $R(T)$, for high-entropy alloy $(\text{ScZrNb})_{0.65}[\text{RhPd}]_{0.35}$ and highly-compressed boron and superhydrides H_3S , LaH_x , PrH_9 and BaH_{12} . In result, we showed that high-entropy alloy $(\text{ScZrNb})_{0.65}[\text{RhPd}]_{0.35}$ exhibited pure electron-phonon mediated superconductor with $p = 4.9 \pm 0.4$. Unexpectedly we revealed that all studied superhydrides exhibit $1.8 < p < 3.2$. This implies that it is unlikely that the electron-phonon interaction is the primary mechanism for the Cooper pairs formation in highly-compressed superhydrides and alternative pairing mechanisms, for instance, the electron-magnon, the electron-polaron, the electron-electron or other, should be considered as the origin for the emerge of near-room-temperature superconductivity in these compounds.

The dominance of non-electron-phonon charge carrier interaction in highly-compressed superhydrides

I. Introduction

The discovery of the first superhydride/superdeuteride superconductor $\text{Th}_4\text{H}_{15}/\text{Th}_4\text{D}_{15}$ by Satterthwaite and Toepke [1] was based on a very clear idea, which they expressed as [1]: “...There has been theoretical speculation [2] that metallic hydrogen might be a high-temperature superconductor, in part because of the very high Debye frequency of the proton lattice. With high concentrations of hydrogen in the metal hydrides one would expect lattice modes of high frequency and if there exists an attractive pairing interaction one might expect to find high-temperature superconductivity in these systems also.”

Surprisingly enough Satterthwaite and Toepke [1] found that isotopic counterparts Th_4H_{15} and Th_4D_{15} have the same superconducting transition temperature, T_c , which is in direct contradiction with the theory of electron-phonon mediated superconductivity [3,4], including the case of hydrogen-rich metallic alloys [5]. Later it was found that PdH-PdD-PdT system exhibits the inverse isotope effect [6,7], where heavier counterparts have higher superconducting transition temperature in comparison with isotopically lighter compounds.

In this regard, we should mention that, despite a milestone experimental discovery reported by Drozdov *et al* [8] on the near-room-temperature superconductivity (NRTS) in highly-compressed sulphur hydride, recent report by Minkov *et al* [9] showed that the isotope effect in $\text{H}_3\text{S}-\text{D}_3\text{S}$ system is not as prominent as it was initially reported [8] in 2015. Primary open question here is what exact stoichiometry of the hydrogen isotopes in NRTS samples. There are some experimental evidences [10] that hydrogen- and deuterium-based NRTS phases have different hydrogen isotopes stoichiometry and, thus, it is possible that the observed difference in T_c for isotopic counterparts is originated from the stoichiometry, rather than from the fundamental difference in the phonon spectra.

Because the charge carriers can form the Cooper pairs not only by the attractive electron-phonon interaction [11,12], there is a necessity to reaffirm or disprove the electron-phonon mediated superconductivity in the NRTS superhydrides. In attempt to do this, here we analysed the temperature dependent resistance, $R(T)$, in several highly-compressed superhydrides by using generalized Bloch-Grüneisen (BG) equation [13,14].

In the result we showed the dominance of non-electron-phonon charge carrier interactions (in particular, the electron-magnon and the electron-electron interactions) in highly-compressed H_3S , LaH_x , PrH_9 , CeH_9 , and BaH_{12} superhydrides. This result is in a good accord with the reports [15,16] where it was shown that NRTS superconductors are in the unconventional superconductors band in the Uemura plot [17,18]. This implies that superhydride superconductors exhibit a non-electron-phonon pairing mechanism.

2. Model description

To determine the type of the charge carrier interaction in NRTS here we proposed to use advanced the Bloch-Grüneisen (BG) equation [13,14] which can be represented in the most general form of [19]:

$$R(T) = R_0 + A_1 \cdot T + \sum_n^{2,3,5} A_p \cdot \left(\frac{T}{T_\theta}\right)^p \cdot \int_{\frac{T_{min}}{T_\theta}}^{\frac{T_\theta}{T}} \frac{x^p}{(e^x-1) \cdot (1-e^{-x})} \cdot dx \quad (1)$$

where R_0 is the resistance at $T \rightarrow 0$ K, T_θ is the Debye temperature, A_p is weighting parameters, T_{min} is lowest temperature at which measurements performed and p is the power-law exponent which has theoretical integer value for following interaction mechanism [19]:

$$p = \begin{cases} 2 & \text{for the electron - electron interaction} \\ 3 & \text{for the electron - magnon interaction} \\ 5 & \text{for the electron - phonon interaction} \end{cases} \quad (2)$$

However, as it is pointed in Ref. 20, the Eq. 1 has a linear limit for $p \rightarrow 1$:

$$\lim_{p \rightarrow 1} \left(\frac{T}{T_\theta} \right)^p \cdot \int_{\frac{T_{min}}{T_\theta}}^{\frac{T_\theta}{T}} \frac{x^p}{(e^x - 1) \cdot (1 - e^{-x})} \cdot dx \rightarrow B \cdot T \quad (3)$$

where B is a constant. Thus, linear term in Eq. 1 can be represented as an integral part at $p \rightarrow 1$ with weighting factor A_1 :

$$R(T) = R_0 + \sum_p \left(\lim_{p \rightarrow 1} \right)^{2,3,5} A_p \cdot \left(\frac{T}{T_\theta} \right)^p \cdot \int_{\frac{T_{min}}{T_\theta}}^{\frac{T_\theta}{T}} \frac{x^p}{(e^x - 1) \cdot (1 - e^{-x})} \cdot dx \quad (4)$$

We should stress that Eq. 4 was never applied for the analysis of experimental $R(T)$ data, because there is a sum of integrals and, thus, the fitting procedure is over-parametrized. However, to the best author's knowledge, in all published work (except, the work by Jiang *et al* [21] and recent report [20]) Eq. 4 was used for the electron-phonon integrand, i.e. $p = 5$ (see, for instance, [22-24]).

One of possible way to use Eq. 4 is to reduce the number of integrals to one, but in this integral the power-law exponent, p , will be a free-fitting parameter:

$$R(T) = R_0 + A_p \cdot \left(\frac{T}{T_\omega} \right)^p \cdot \int_{\frac{T_{min}}{T_\omega}}^{\frac{T_\omega}{T}} \frac{x^p}{(e^x - 1) \cdot (1 - e^{-x})} \cdot dx \quad (5)$$

where we introduce the designation of T_ω for the characteristic temperature for the case when p is free-fitting parameter, while the designation of T_θ is remained for $p = 5$.

Thus, the dominant charge carrier interaction mechanism in given materials can be determined from the deduced by the comparison of the deduced free-fitting parameter p with theoretical values for pure cases (Eq. 2).

From the best author's knowledge, Eq. 5 was first used by Jiang *et al* [21] to reveal the dominant interaction mechanism in $\text{Sr}_2\text{Cr}_3\text{As}_2\text{O}_2$ ferrimagnet. In result, the mechanism was revealed as the electron-magnon (with deduced $p = 3.34$ [21]), which was the first confirmation of the approach validity. More recently, in Ref. 20, the approach was applied for pure copper, iron and cobalt (for which $R(T)$ was reported by White and Woods [25]), as well as for the electron-phonon mediated superconductor ReBe_{22} (for which $R(T)$ was reported by

Shang *et al* [22]), highly-compressed superconducting ε -phase of iron (for which $R(T)$ was reported by Shimizu *et al* [26] and by Jaccard *et al* [27]), and twisted bilayer graphene superlattice (for which $R(T)$ was reported by Polshin *et al* [28]).

Here to fit $R(T)$ data we used recently proposed equation [29]:

$$R(T) = R_0 + \theta(T_c^{onset} - T) \cdot \left(\frac{R_{norm}}{\left(I_0 \left(F \cdot \left(1 - \frac{T}{T_c^{onset}} \right)^{3/2} \right) \right)^2} \right) + \theta(T - T_c^{onset}) \cdot \left(R_{norm} + A \cdot \left(\left(\frac{T}{T_\omega} \right)^p \cdot \int_{\frac{T_{min}}{T_\omega}}^{\frac{T_\omega}{T}} \frac{x^p}{(e^x - 1) \cdot (1 - e^{-x})} \cdot dx - \left(\frac{T_c^{onset}}{T_\omega} \right)^p \cdot \int_{\frac{T_{min}}{T_\omega}}^{\frac{T_c^{onset}}{T_\omega}} \frac{x^p}{(e^x - 1) \cdot (1 - e^{-x})} \cdot dx \right) \right) \quad (6)$$

where instead of fixed $p = 5$ (as it was the case in Ref. 29), here we used p as a free-fitting parameter, T_c^{onset} is free-fitting parameter designated the onset of superconducting transition, R_{norm} is the sample resistance at the onset of the transition, $\theta(x)$ is the Heaviside step function, $I_0(x)$ is the zero-order modified Bessel function of the first kind and F is a free-fitting dimensionless parameter. More details about Eq. 6 (for the case of fixed $p = 5$) can be found elsewhere [29,30].

3. Results and discussion

3.1. High-entropy alloy (ScZrNb)_{0.65}[RhPd]_{0.35}

Because Eq. 5 has been applied for limited range of materials to date [20,21], there is a necessity to show that the approach is widely applicable. Here we applied Eq. 5 to fit $R(T)$ data for high-entropy alloy (ScZrNb)_{0.65}[RhPd]_{0.35} for which raw experimental $R(T)$ data was reported by Stolze *et al* [31]. It should be mentioned that recently we fitted this $R(T)$ dataset to Eq. 5 for fixed $p = 5$ [29], and here we make p parameter to be free. In Fig. 1 we show the fit of $R(T)$ data to Eq. 5 for which deduced $p = 4.9 \pm 0.4$. This implies that the

superconducting state in high-entropy alloy $(\text{ScZrNb})_{0.65}[\text{RhPd}]_{0.35}$ emerges solely from the electron-phonon interaction.

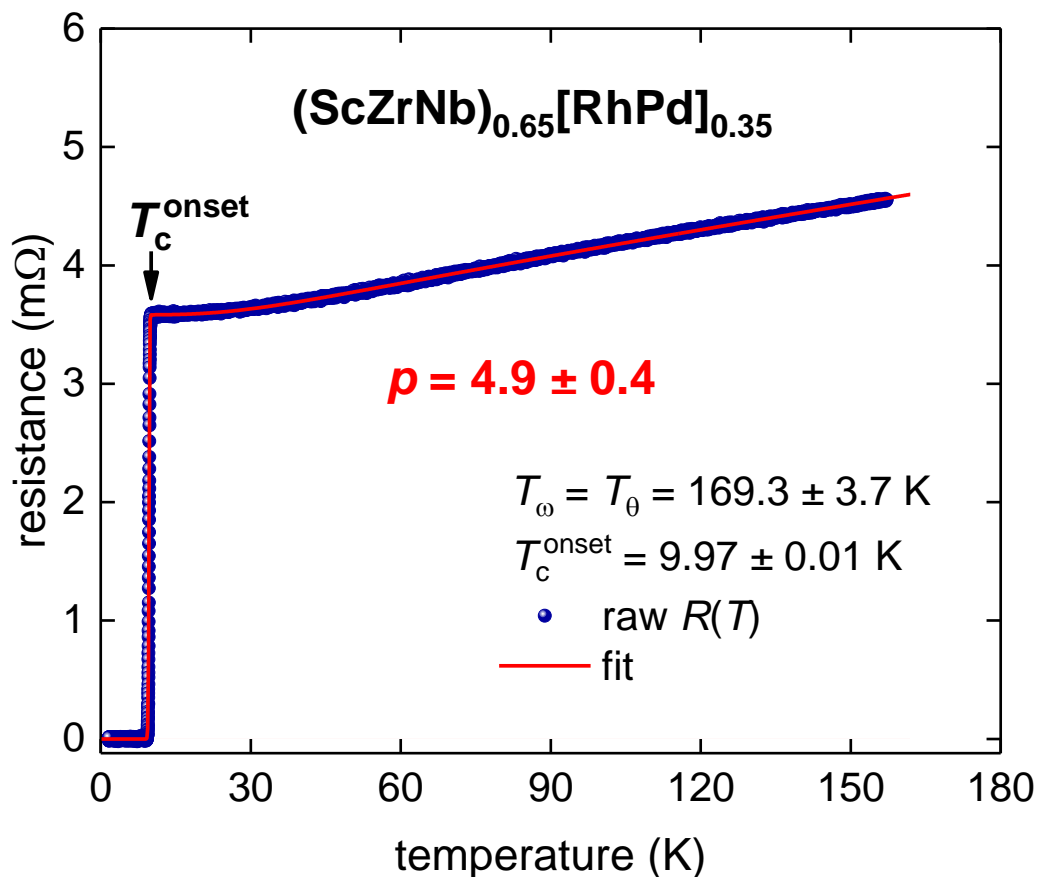


Figure 1. $R(T)$ data for high-entropy alloy $(\text{ScZrNb})_{0.65}[\text{RhPd}]_{0.35}$ reported by Stolze *et al* [31] and data fit to Eq. 5. Green ball shows $T_{c,0.03}$ defined by $\frac{R(T)}{R(T_c^{\text{onset}}) - R_0} = 0.03$ criterion. 95% confidence bars are narrower than the fitting curve. Goodness of fit is 0.99997.

3.2. α -Ga phase of highly-compressed boron

Now we turn to highly-compressed superconductors and in Fig. 2 we showed $R(T)$ data for elemental boron pressurized at $P = 240 \text{ GPa}$ (reported by Erements *et al* [32]). Oganov *et al* [33] showed that elemental boron at pressure above $P = 89 \text{ GPa}$ exhibits in so-called α -Ga phase and, thus, the superconducting state emerges in this boron phase. It should be stressed that the fit to Eq. 5 can be also performed also for fixed $p = 5$ value (Fig. 2,a). This fit has a

high quality (the goodness of fit is 0.9977) and deduced $T_\theta = 318 \pm 7$ K is in expected range.

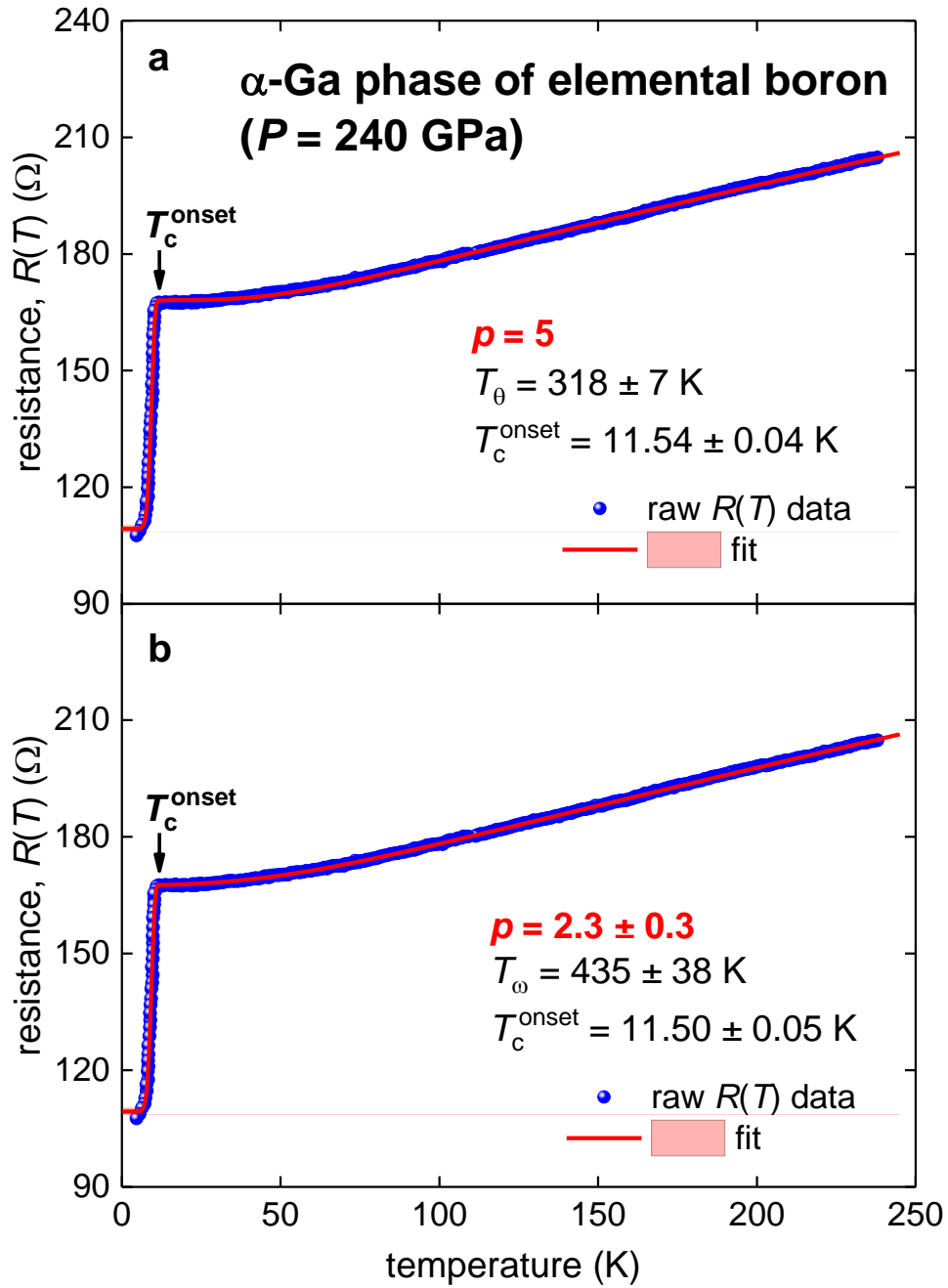


Figure 2. Resistance data, $R(T)$, and fit to Eq. 5 for highly-compressed elemental boron (raw data reported by Eremets *et al* [32]). 95% confidence bars are shown by pink shaded area. (a) $p = 5$ (fixed); goodness of fit is 0.9977. (b) $p = 2.3 \pm 0.3$; goodness of fit is 0.9978.

However, when p was chosen to be free-fitting parameter, the deduced value $p = 2.3 \pm 0.3$ indicate that the electron-electron interaction is the dominant in this superconductor. To

explain this unexpected result, one can take in account that elemental boron is situated between metals and insulators in the Mendeleev's table. Despite this element exhibits three valence electrons, which are, in principles, can lead to the metallic conductivity, the electrons are sufficiently localized and at ambient conditions the boron is an insulator [33]. Thus, there is not a really surprize, that the electron-electron interaction dominates in this materials even at high-pressure.

3.3. *Im-3m*-phase of highly-compressed H₃S

Mozaffari *et al* [34] in their Fig. 1 reported $R(T)$ curves for *Im-3m*-H₃S sample subjected to pressure of $P = 155 \text{ GPa}$ and of $P = 160 \text{ GPa}$. In Fig. 3 we showed $R(T)$ curve and data fit to Eq. 5 for sample designated by Mozaffari *et al.* [34] as **155 GPa: 07/2018**. It can be seen (Fig. 3), that fit to Eq. 5 at fixed $p = 5$ (Fig. 3,a) exhibits a high quality and deduced $T_{\theta} = 1427 \pm 2 \text{ K}$ is in a good agreement with respectful characteristic temperatures for the phonon spectrum reported by first-principles calculations for this compound [35-41]. However, in the case of p is a free-fitting parameter, its value is reduced to the close proximity to the electron-electron interaction value of $p = 2.44 \pm 0.03$.

This result can be explained as a manifestation of the covalent-like atomic bonds between ions in *Im-3m*-phase of H₃S. Detailed discussion of this feature of highly-pressurized sulfur hydride can be found elsewhere [42].

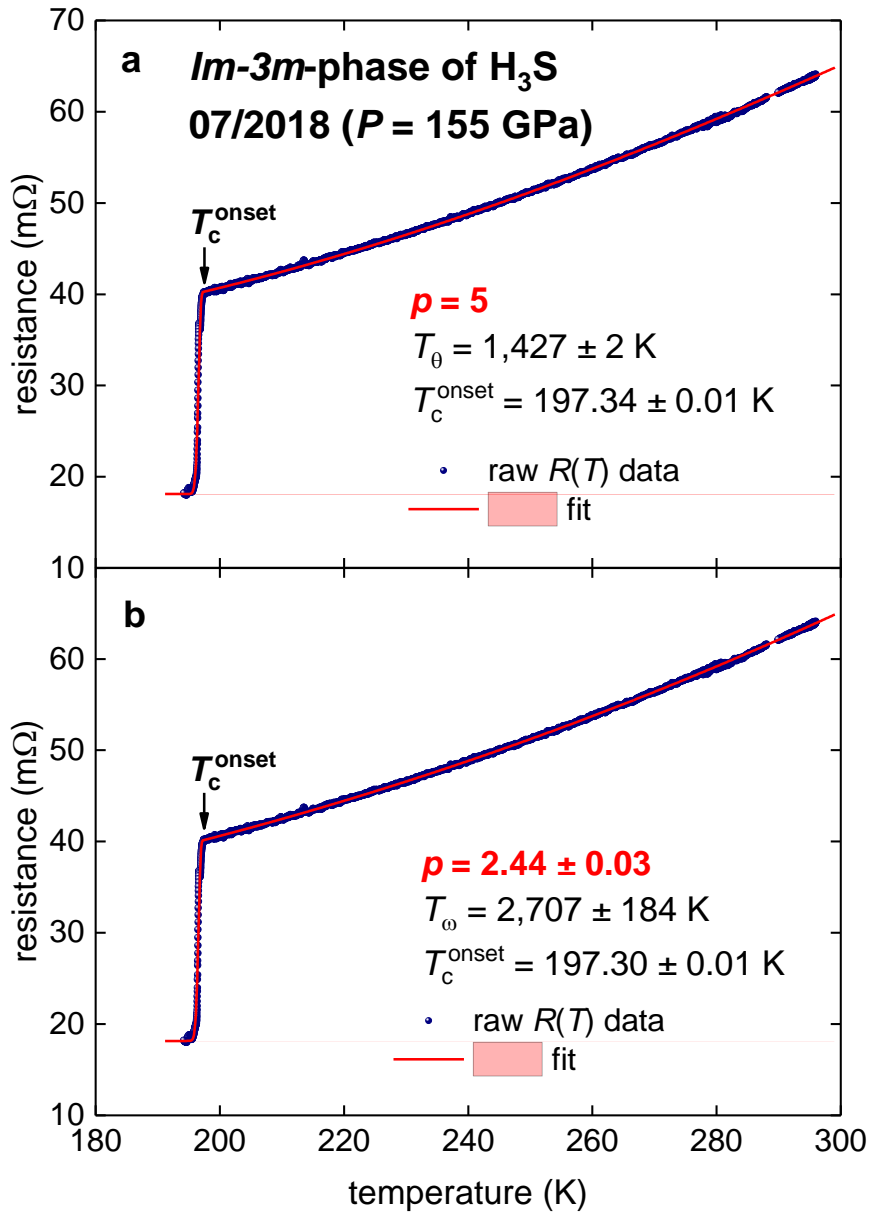


Figure 3. Resistance data, $R(T)$, and fit to Eq. 5 for highly-compressed *Im-3m*-H₃S phase (raw data reported by Mozaffari *et al* [34]). 95% confidence bars are narrower than the fitting curve. (a) $p = 5$ (fixed); goodness of fit is 0.9994. (b) $p = 2.44 \pm 0.03$; goodness of fit is 0.9995.

3.4. Highly-compressed LaH_x ($P = 150$ GPa)

Drozdov *et al* [43] reported on the discovery of NRT superconductivity in highly-compressed lanthanum hydride, *Fm-3m*-phase of LaH₁₀. Due to the highest temperature at which $R(T)$ data is measured for all NRTS compounds is limited by 300 K, there is no possibility to fit $R(T)$ data measured for *Fm-3m*-LaH₁₀ samples (which all exhibited $T_c \sim 250$

K), because of the narrow temperature range for which $R(T)$ curves have non-zero values.

However, $R(T)$ data for Sample 11 designated as hydrogen deficient LaH_x (where $x > 3$) with $T_c \sim 70$ K can be reliably fitted to Eq. 5. The fits for $p = 5$ and for p to be a free-fitting parameter are shown in Fig. 4.

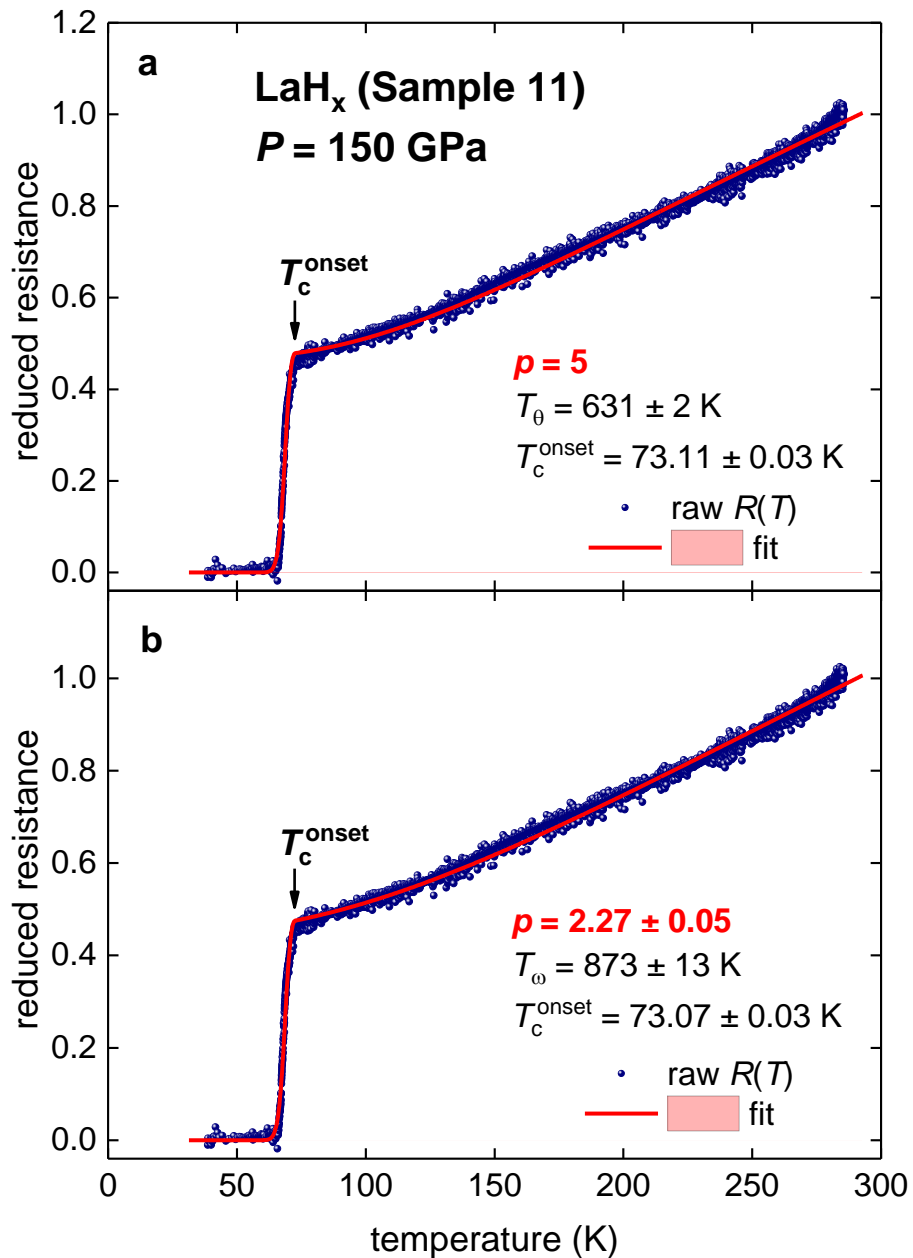


Figure 4. $R(T)$ data and fit to Eq. 5 for highly-compressed hydrogen deficient LaH_x ($x > 3$, Sample 11 [43]). (a) $p = 5$ (fixed); fit quality 0.9965; (b) $p = 2.27 \pm 0.05$; fit quality 0.9970.

It can be seen in Fig. 4, that again as for highly-compressed boron and H3S, Sample 11 of LaH_x exhibits dominant the electron-electron charge carrier interaction. We can point out that

the electron-electron charge carrier interaction in LaH_x is more likely originated from the covalent-like atomic bonds.

3.5. Highly-compressed $F-43m\text{-PrH}_9$ and $P6_3/mmc\text{-PrH}_9$

Zhou *et al* [44] reported the discovery of low- T_c superconductivity in highly-compressed praseodymium hydride. All synthesized samples contained a mixture of $F-43m\text{-PrH}_9$ and $P6_3/mmc\text{-PrH}_9$ phases. In Figure 5 we show the fits of $R(T)$ measured at different pressure in the range of ($P = 135\text{-}145$ GPa [44]).

In studied pressure range free-fitted parameter p is varied in the range of $1.80 \leq p \leq 1.99$. This p range is close to the theoretical value for pure electron-electron interaction.

3.6. Highly-compressed pseudocubic BaH_{12}

Chen *et al* [45] reported the discovery of low- T_c superconductivity in highly-compressed barium hydride BaH_{12} which exhibited pseudocubic crystalline structure to be subjected to pressure from 75 to 173 GPa. Here we analysed $R(T)$ curves (showed in Fig. S41(c) [45]) for the sample subjected to the pressure of $P = 100$ GPa and was a subjected to two consequent laser annealing/heating. In Figures 6 we show $R(T)$ data and the fit to Eq. 5 for laser annealing/heating #1. It can be seen (Fig. 6,a) that $R(T)$ can be with a very good quality fitted for fixed $p = 5$ value. However, when p is free-fitting parameter it decreased to the value close to pure case for the electron-magnon interaction.

3.7. Discussion

In overall, in all considered highly-compressed superconductors, i.e. $\alpha\text{-Ga}$ phase of boron, H_3S , LaH_x , PrH_9 , BaH_{12} and $\epsilon\text{-phase}$ of Fe (considered in Ref. 20), we have found essentially the same result that power-law exponent, p , in generalized Bloch-Grüneisen (BG)

equation (Eq. 5) is well below 5, i.e. the value designated for pure electron-phonon charge carrier interaction.

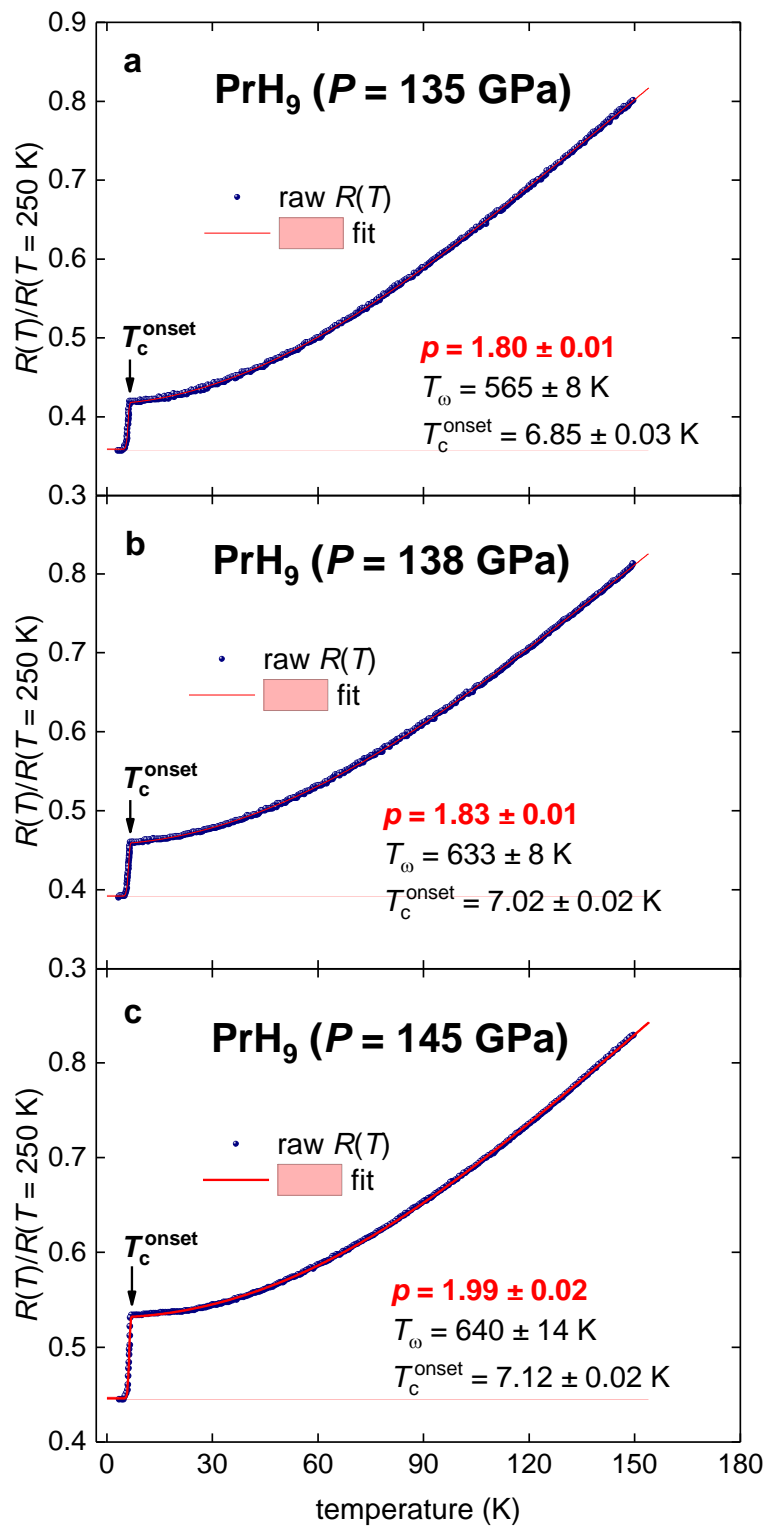


Figure 5. $R(T)$ data for highly-compressed PrH₉ ($P = 135\text{-}145$ GPa [44]) and data fits to Eq. 5. (a) $P = 135$ GPa, $p = 1.80 \pm 0.01$; fit quality 0.9998. (b) $P = 138$ GPa, $p = 1.83 \pm 0.01$; fit quality 0.9998. (c) $P = 145$ GPa, $p = 1.99 \pm 0.02$; fit quality 0.9997.

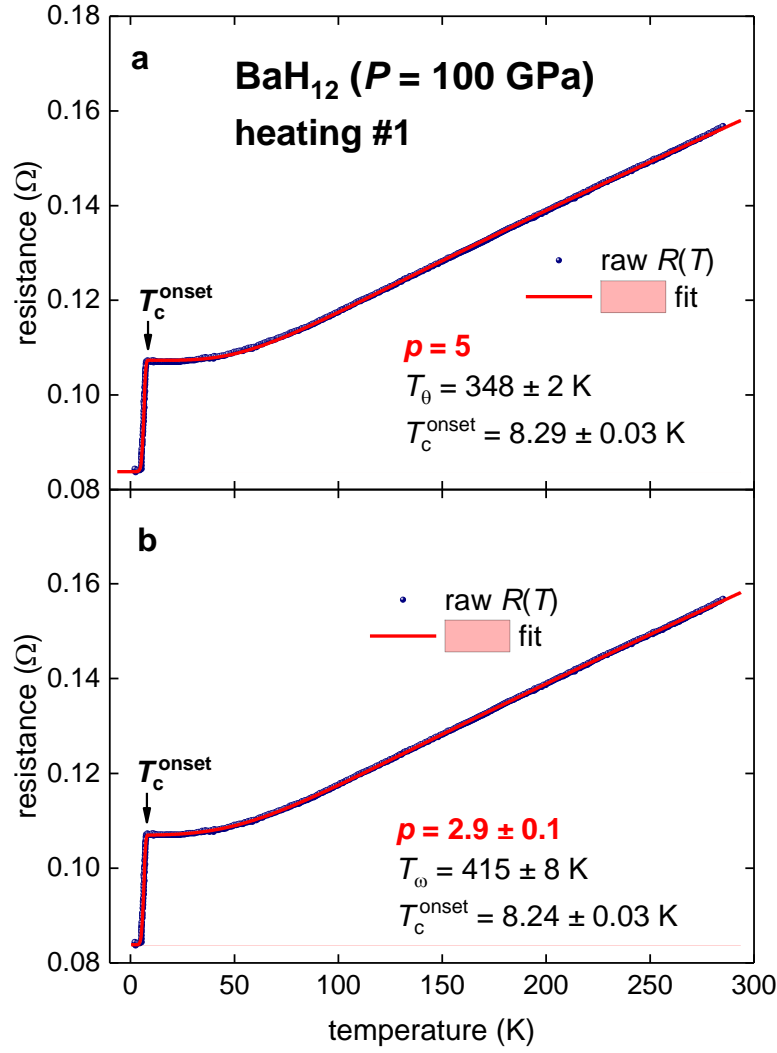


Figure 6. $R(T)$ data for highly-compressed BaH_{12} (heating #1, $P = 100$ GPa [45]) and data fits to Eq. 5. (a) $p = 5$ (fixed); fit quality 0.9996; (b) $p = 2.9 \pm 0.1$; fit quality 0.9997.

From other hand, for two conventional superconductors ReBe_{22} [20] and high-entropy alloy $(\text{ScZrNb})_{0.65}[\text{RhPd}]_{0.35}$ (Fig. 1) deduced free-fitting parameter p is practically undistinguishable from 5. This implies that while the electron-phonon interaction is primary mechanism for the emerge of the superconductivity in ReBe_{22} and $(\text{ScZrNb})_{0.65}[\text{RhPd}]_{0.35}$, all highly-compressed superconductors exhibit different charge carrier pairing mechanism.

It should be mentioned that there are many theoretically possible mechanisms for the charge carriers pairing in the condensed matter [11,46], and from deduced power-law exponent presented herein, it is more likely that primary mechanism is related to the electron-

electron interaction. This finding is in a good accord with empirical finding that all hydrogen-rich superconductors are located [15,16,47] in unconventional superconductors band in the Uemura plot [17,18].

Taking in account a possible argument that the first-principles calculations have predicted reasonably accurate the superconducting transition temperature in several (and what is important to stress, not in all) hydrogen-rich superconductors, the discussion can be related to the issue that sufficiently strong electron-phonon interaction can be accommodated consequence of strong electron-electron interaction. Thus, by varying the Coulomb pseudopotential parameter, μ^* , and the electron-phonon coupling constant, λ_{e-ph} , in equations similar to ones proposed by McMillan [48], and Allen and Dynes [49-51]:

$$T_c = \left(\frac{1}{1.20}\right) \cdot \left(\frac{\hbar}{k_B}\right) \cdot \omega_{ln} \cdot e^{-\left(\frac{1.04 \cdot (1 + \lambda_{e-ph})}{\lambda_{e-ph} - \mu^* \cdot (1 + 0.62 \cdot \lambda_{e-ph})}\right)} \cdot f_1 \cdot f_2 \quad (6)$$

where k_B is the Boltzmann constant, and \hbar is reduced Planck constant, ω_{ln} is logarithmic phonon frequency, and f_1 and f_2 are correction functions, it is possible to find correlative dependence between primary mechanism (which is non-electron-phonon) with the associated electron-phonon interaction.

5. Conclusions

In conclusion, in this paper we analysed $R(T)$ data for high-entropy alloy $(\text{ScZrNb})_{0.65}[\text{RhPd}]_{0.35}$, and highly-compressed α -Ga phase of boron, H_3S , LaH_x , PrH_9 and BaH_{12} and showed that the dominant charge carrier interaction in studied highly-compressed superconductors has non-electron-phonon nature.

Acknowledgement

The author thanks Mr. A. V. Nikitin (M.N. Mikheev Institute of Metal Physics) for fruitful discussion and valuable correction in mathematical expression of Eq. 5. The author thanks Dr. K. Stolze (Leibniz-Institut für Kristallzüchtung) for providing $R(T)$ data for high-entropy alloy $(\text{ScZrNb})_{0.65}[\text{RhPd}]_{0.35}$, Dr. M. I. Eremets and Dr. V. S. Minkov (Max-Planck Institut für Chemie, Mainz, Germany) for providing data for $Fm-3m$ -phase of lanthanum hydride, and Dr. S. Mozafarri and co-authors (National High Magnetic Field Laboratory, Florida State University, USA) for open access magnetoresistance data for $Im-3m$ -phase of H_3S [34].

The author thanks financial support provided by the Ministry of Science and Higher Education of Russia (theme “Pressure” No. AAAA-A18-118020190104-3) and by Act 211 Government of the Russian Federation, contract No. 02.A03.21.0006.

References

- [1] Satterthwaite C B and Toepke I L 1970 Superconductivity of hydrides and deuterides of thorium *Phys. Rev. Lett.* **25** 741-743
- [2] Ashcroft N W 1968 Metallic hydrogen: a high-temperature superconductor? *Phys. Rev. Lett.* **21** 1748-1749
- [3] Bardeen J, Cooper L N, and Schrieffer J R 1957 Theory of superconductivity *Phys. Rev.* **108** 1175-1204
- [4] Eliashberg G M 1960 Interactions between electrons and lattice vibrations in a superconductor *Soviet Phys. JETP* **11** 696-702
- [5] Ashcroft N W 2004 Hydrogen dominant metallic alloys: high temperature superconductors? *Phys. Rev. Lett.* **92** 187002
- [6] Stritzker B and Buckel W 1972 Superconductivity in the palladium-hydrogen and the palladium-deuterium systems *Zeitschrift für Physik A Hadrons and nuclei* **257** 1-8
- [7] Yussouff M, Rao B K and Jena P 1995 Reverse isotope effect on the superconductivity of PdH, PdD, and PdT *Solid State Communications* **94** 549-553
- [8] Drozdov A P, Eremets M I, Troyan I A, Ksenofontov V, Shylin S I 2015 Conventional superconductivity at 203 kelvin at high pressures in the sulfur hydride system *Nature* **525** 73-76
- [9] Minkov V S, Prakapenka V B, Greenberg E and Eremets M I 2020 Boosted T_c of 166 K in superconducting D_3S synthesized from elemental sulfur and hydrogen *Angew. Chem. Int. Ed.* **59** 18970-18974
- [10] Drozdov A P, *et al* 2019 Superconductivity at 250 K in lanthanum hydride under high pressures *Nature* **569** 528-531

- [11] Monthoux P, Pines D and Lonzarich G G 2007 Superconductivity without phonons *Nature* **450** 1177-1183
- [12] Sachdev S 2012 What can gauge-gravity duality teach us about condensed matter physics? *Annual Review of Condensed Matter Physics* **3** 9-33
- [13] Bloch F 1930 Zum elektrischen Widerstandsgesetz bei tiefen Temperaturen *Z. Phys.* **59** 208-214
- [14] Grüneisen E 1933 Die abhängigkeit des elektrischen widerstandes reiner metalle von der temperatur. *Ann. Phys.* **408** 530–540
- [15] Talantsev E F 2019 Classifying superconductivity in compressed H₃S *Modern Physics Letters B* **33** 1950195
- [16] Talantsev E F 2020 An approach to identifying unconventional superconductivity in highly-compressed superconductors *Superconductor Science and Technology* **33** 124001
- [17] Uemura Y J 1997 Bose-Einstein to BCS crossover picture for high- T_c cuprates *Physica C* **282-287** 194-197
- [18] Uemura Y J 2019 Dynamic superconductivity responses in photoexcited optical conductivity and Nernst effect *Phys. Rev. Materials* **3** 104801
- [19] Poker D B and Klabunde C E 1982 Temperature dependence of electrical resistivity of vanadium, platinum, and copper *Phys. Rev. B* **26** 7012
- [20] Talantsev E 2021 Quantifying the charge carrier interaction in metallic twisted graphene superlattices arXiv:2103.04810
- [21] Jiang H, *et al* 2015 Physical properties and electronic structure of Sr₂Cr₃As₂O₂ containing CrO₂ and Cr₂As₂ square-planar lattices *Phys. Rev. B* **92** 205107
- [22] Shang T, *et al* 2019 Enhanced T_c and multiband superconductivity in the fully-gapped ReBe₂₂ superconductor *New J. Phys.* **21** 073034
- [23] Barker J A T, *et al* 2018 Superconducting and normal-state properties of the noncentrosymmetric superconductor Re₃Ta *Phys. Rev. B* **98** 104506
- [24] Matsumoto R, *et al* 2019 Pressure-induced superconductivity in tin sulphide *Phys. Rev. B* **99** 184502
- [25] White G K and Woods S B 1959 Electrical and thermal resistivity of the transition elements at low temperatures *Phil. Trans. R. Soc. Lond. A* **251**, 273-302
- [26] Shimizu K, *et al* 2001 Superconductivity in the nonmagnetic state of iron under pressure *Nature* **412** 316-318
- [27] Jaccard D, *et al* 2002 Superconductivity of ϵ -Fe: complete resistive transition *Physics Letters A* **299** 282-286
- [28] Polshyn H, *et al* 2019 Large linear-in-temperature resistivity in twisted bilayer graphene *Nature Physics* **15** 1011
- [29] Talantsev E F and Stolze K 2021 Resistive transition in hydrogen-rich superconductors *Superconductor Science and Technology* **34** 064001
- [30] Talantsev E F 2020 Advanced McMillan's equation and its application for the analysis of highly-compressed superconductors *Superconductor Science and Technology* **33** 094009
- [31] Stolze K, Tao J, von Rohr F O, Kong T, Cava R J 2018 Sc–Zr–Nb–Rh–Pd and Sc–Zr–Nb–Ta–Rh–Pd high-entropy alloy superconductors on a CsCl-type lattice *Chem. Mater.* **30** 906-914
- [32] Eremets M I, Struzhkin V V, Mao H-K, Hemley R J 2001 Superconductivity in boron *Science* **293** 272-274
- [33] Oganov A R, *et al* 2009 Ionic high-pressure form of elemental boron *Nature* **457** 863-867
- [34] Mozaffari S, *et al* 2019 Superconducting phase diagram of H₃S under high magnetic fields *Nature Communications* **10** 2522

- [35] Li Y, *et al* 2014 The metallization and superconductivity of dense hydrogen sulfide *The Journal of Chemical Physics* **140** 174712
- [36] Duan D, *et al* 2015 Pressure-induced metallization of dense $(\text{H}_2\text{S})_2\text{H}_2$ with high- T_c superconductivity *Scientific Reports* **4** 6968
- [37] Duan D, *et al* 2015 Pressure-induced decomposition of solid hydrogen sulphide *Phys. Rev. B* **91** 180502
- [38] Errea I *et al* 2015 High-pressure hydrogen sulfide from first principles: A strongly anharmonic phonon-mediated superconductor *Phys. Rev. Lett.* **114** 157004
- [39] Durajski A P 2016 Quantitative analysis of nonadiabatic effects in dense H_3S and PH_3 superconductors *Sci. Rep.* **6** 38570
- [40] Goncharov A F, Lobanov S S, Kruglov I, Zhao X-M, Chen X-J, Oganov A R, Konopkova Z, Prakapenka V B 2016 Hydrogen sulfide at high pressure: Change in stoichiometry *Phys. Rev. B* **93** 174105
- [41] Zureka E and Bi T 2019 High-temperature superconductivity in alkaline and rare earth polyhydrides at high pressure: A theoretical perspective *J. Chem. Phys.* **150** 050901
- [42] Gor'kov L P and Kresin V Z 2018 Colloquium: High pressure and road to room temperature superconductivity *Review of Modern Physics* **90** 011001
- [43] Drozdov A P, *et al* 2019 Superconductivity at 250 K in lanthanum hydride under high pressures *Nature* **569** 528-531
- [44] Zhou D, *et al* 2020 Superconducting praseodymium superhydrides *Science Advances* **6** eaax6849
- [45] Chen W, *et al* 2021 Synthesis of molecular metallic barium superhydride: pseudocubic BaH_{12} *Nature Communications* **12** 273
- [46] Matthias B T 1971 Anticorrelations in superconductivity *Physica* **55** 69-72
- [47] Talantsev E F 2019 Classifying hydrogen-rich superconductors *Materials Research Express* **6** 106002
- [48] McMillan W L 1968 Transition temperature of strong-coupled superconductors *Phys. Rev.* **167** 331-344
- [49] Dynes R C 1972 McMillan's equation and the T_c of superconductors *Solid State Communications* **10** 615-618
- [50] Allen P B and Dynes R C 1975 Transition temperature of strong-coupled superconductors reanalysed *Phys. Rev. B* **12** 905-922
- [51] Allen P B, in *Handbook of Superconductivity* (edited by C. P. Poole, Jr.) (Academic Press, New York, 1999) Ch. 9, Sec. G, pp. 478-489